Vaccine 37 (2019) 6022–6029

Contents lists available at ScienceDirect

Vaccine

journal homepage: www.elsevier.com/locate/vaccine

Structural and antigenic characterization of a computationally-optimized H5 hemagglutinin influenza vaccine

Yael Bar-Peled [a,1], Jiachen Huang [a,b,1], Ivette A. Nuñez [a,b], Spencer R. Pierce [a], Jeffrey W. Ecker [a], Ted M. Ross [a,b], Jarrod J. Mousa [a,b,*]

[a] Center for Vaccines and Immunology, College of Veterinary Medicine, University of Georgia, Athens, GA 30602, United States
[b] Department of Infectious Diseases, College of Veterinary Medicine, University of Georgia, Athens, GA 30602, United States

ARTICLE INFO

Article history:
Received 13 April 2019
Received in revised form 16 August 2019
Accepted 25 August 2019
Available online 31 August 2019

Keywords:
Influenza
Vaccine
Antibody
Hemagglutinin

ABSTRACT

Influenza A virus is a leading cause of death worldwide. Viruses of the H5 subtype have the potential to induce high mortality, and no vaccines are currently available to protect against H5 influenza viruses in the event of an outbreak. Experimental vaccination with one clade 2 virus does not protect against other subclades. The computationally optimized broadly reactive (COBRA) methodology was previously used to generate a H5 hemagglutinin (HA) antigen (COBRA2) that elicited increased serological breadth against multiple clade 2 H5N1 influenza viruses. In this report, we structurally and antigenically characterized the COBRA2 HA antigen. We examined the biochemical characteristics of the COBRA2 protein and determined the protein is correctly cleaved, properly folded into a trimeric structure, and antigenically correct by probing with HA head- and stem-specific monoclonal antibodies (mAbs). We further probed the antigenicity by examining binding of a panel of H5 mouse mAbs to the COBRA2 antigen, as well as several other HA antigens. We determined the X-ray crystal structure of the COBRA2 HA antigen to 2.8 Å and the protein was observed to be in the expected trimeric form. The COBRA2 HA was structurally similar to the naturally occurring H5 HA antigens and suggests the protein folds similar to known HA structures. Overall, our data allow us to formulate a hypothesis on the mechanism of increased breadth due to vaccination with the COBRA2 HA antigen, which is that the protein incorporates antigenic sites from numerous HA antigens, and elicits mAbs with limited breadth, but with diversity in targeted antigenic sites.

1. Introduction

Influenza virus is a leading global pathogen with the potential to cause large-scale pandemics in human and animal populations [1]. The 1918 [2] and 2009 [3] H1N1 influenza viruses, which exhibited wide-spread infections across the world, are prime examples of the ability of influenza virus to quickly spread worldwide, and, in the case of the 1918 pandemic, to cause tens of millions of deaths across the globe. Another subtype of influenza with the potential to cause a pandemic are those viruses containing H5 hemagglutinin (HA) antigens. In particular, H5N1 is a highly pathogenic subtype of influenza A that originated from birds, and has caused over 50% mortality in cases of human infection [4]. Although the virus has remained dormant in recent years, H5N1 still poses a potential threat to the world [5]. A H5N2 outbreak in the United States in 2015 caused an enormous impact to the turkey and chicken industry in the midwestern United States [6]. During the 2016–2017 time period, H5N6 and H5N8 cases were frequently reported from east Asia and Europe [7–9]. These highly pathogenic avian influenza viruses still pose a great threat to the world. Currently, there is no report of efficient inter-human transmission of H5N1 influenza viruses, but a H5N1 variant strain serially-passaged in ferrets acquired amino acid mutations in the HA surface protein that enabled the virus to spread between ferrets via aerosol transmission [10]. In addition, H5N1 influenza viruses are genetically compatible with human pandemic strains including H1N1 and H3N2 [11]. Wild birds are a natural reservoir for influenza viruses, and with frequent mutations and viral reassortment events, there is the potential for a recurrence of more virulent and transmissible H5 influenza strains [12].

Vaccination is the best approach to prevent influenza virus infection. However, there is currently no commercial vaccine for H5N1 available for humans. For influenza virus, the grand challenge for the scientific community is to develop effective vaccines that overcome the antigenic diversity of these viruses. Based on the phylogenetic distance of HA genes, ten different H5 HA clades have

* Corresponding author.
E-mail address: jarrod.mousa@uga.edu (J.J. Mousa).
[1] Contributed equally.

https://doi.org/10.1016/j.vaccine.2019.08.062
0264-410X/

been identified [12]. Among them, clade 2 covers a large percentage of strains that circulate and have been isolated from birds and humans in >60 countries [13]. Although the HA sequences within branches of clade 2 are over 90% similar, the receptor-blocking antibody cross-reactivity elicited by these strains is poor [14]. Current seasonal influenza vaccines utilize a polyvalent formulation to cover the most prevalent circulating strains. However, in some seasons, the prevalent strains circulating several months later are antigenically different from the vaccine selected strains [15]. In order to develop an improved seasonal influenza vaccine, a new strategy termed computationally optimized broadly reactive antigen (COBRA) was used to generate HA antigens that elicit antibodies with neutralizing activity against a broad number of co-circulating viruses per subtype [16–18]. The Human COBRA 2 HA (COBRA2) antigen, was derived from layering 129 unique H5 HA sequences [16]. The sequences represent clade 2 H5N1 viruses isolated from human infections between 2004 and 2006. Vaccine candidates were generated from human H5N1 clade 2 HA sequences by several rounds of consensus building, and the most representative amino acid at each position was incorporated to form the final sequence [16]. This vaccine candidate successfully broadened protection against numerous influenza strains in mice, ferrets, and non-human primates [17,19–21].

The mechanism by which the COBRA2 HA antigen elicits a broadly-reactive antibody response compared to H5 HA antigens derived from wild-type H5N1 strains is unknown. The overall conformation and fine-structural details of the COBRA2 HA antigen need to be determined to identify the structural homology to naturally-occurring H5 sequences, and to inform the mechanism of increased serological breadth. Therefore, in this study, the crystal structure of the H5 COBRA2 HA antigen was determined, and antigenic characteristics were probed using a panel of H5-specific monoclonal antibodies (mAbs). Overall, the crystal structure of COBRA2 HA revealed structural insights into the COBRA2 HA vaccine mechanism of serological breadth.

2. Materials and methods

2.1. Expression of H5 HA influenza proteins.

The COBRA2 HA gene was derived using computationally optimized broadly reactive antigen methodology as previously described [16]. The full HA open reading frame encoding for the COBRA2 gene was modified using site directed mutagenesis to alter the tyrosine at amino acid residue 91 to a phenylalanine (Y91F). The final gene cassette consisted of the extracellular domain of the H5 HA that was C-terminally fused to the trimeric FoldOn domain of T4 fibritin, an AviTag sequence, and a hexahistidine affinity tag [22,23], and subcloned into the mammalian expression vector pcDNA3.1/Zeo(+) (Thermo Fisher Scientific). The protein was recombinantly expressed in Expi293F cells following the manufacturer's protocol. Collected supernatants containing the H5 COBRA2 HA antigen were purified on a HisTrapExcel column and washed and eluted using the AKTA Pure System following the manufacturer's recommended protocol. Eluted fractions were pooled and purified proteins were verified for integrity by probing with an anti-HIS tag antibody (Biolegend, San Diego, CA, USA) via SDS-PAGE and Western blot. Influenza HA-specific mAbs were obtained from BEI Resources and the International Reagent Resource. Influenza A/Vietnam/1203/04 HA1, A/Anhui/1/05, and A/Indonesia/5/05 HA proteins were obtained from the International Reagent Resource.

Biochemical characterization of the COBRA-2 HA protein. To determine if the COBRA2 protein was properly cleaved, SDS-PAGE was utilized. 25 μg of protein per well was loaded onto a 4–12% Bis-Tris protein gel (Thermo Fisher Scientific) in NuPage MES running buffer (Thermo Fisher Scientific). Samples were analyzed in the absence and presence of 1x NuPAGE sample reducing agent (Thermo Fisher Scientific). To determine the oligomeric status of the COBRA-2 protein, 200 μg of protein was analyzed by size exclusion chromatography on a HiLoad Superdex S200 16/600 column (GE Healthcare Life Sciences) in 50 mM Tris pH 7.5, 50 mM NaCl. The column was characterized using the HMW Gel filtration calibration kit (GE Healthcare Life Sciences).

Negative-stain electron microscopy analysis. Trimeric COBRA2 protein isolated following size exclusion chromatography as described above was utilized for analysis by negative-strain electron microscopy. Carbon-coated copper grids were overlaid with the protein at 5 μg/mL for 3 min. The grid was washed in water twice and then stained with 0.75% uranyl formate for 1 min. Negative-stain electron micrographs were acquired using a JEOL JEM1011 TEM microscope equipped with a high contrast 2 k × 2 k AMT mid-mount digital camera using 40,000× magnification.

Deglycosylation of the COBRA2 protein. Recombinant PNGase F was obtained from New England Biolabs. 10 μg of COBRA2 protein was used for both the denaturing and nondenaturing protocols. For the denaturing protocol, the protein was deglycosylated following the manufacturer's protocol. For the nondenaturing protocol, the COBRA2 protein was incubated with 1000 units of PNGase F for 24 h at 37 °C. In the SDS-PAGE mobility shift assay, 2.5 μg of protein was loaded into the untreated lane, while 10 μg of protein was loaded into the deglycosylated denatured and non-denatured gel lanes.

Assays for mAb binding and competition. To perform biolayer interferometry to assess mAb binding and to perform competition assays, we utilized the OctetRED384 system incorporating anti-penta-HIS biosensors. The biosensors were first preincubated for at least 10 min in kinetics buffer (ForteBio, diluted 1:10 in PBS) before obtaining a baseline reading in kinetics buffer. Following this, biosensors were immersed in kinetics buffer containing 10 μg/mL of the COBRA2Y91F protein for 120 s. The baseline signal was measured again in kinetics buffer for 60 s before biosensor tips were immersed into wells containing 100 μg/mL primary antibody for 300 s. For dissociation, the biosensors were returned to kinetics buffer, and for competition the biosensors were moved to a solution of the competing mAb at 100 μg/mL in kinetics buffer. For analysis of competition data, the percent binding of the second mAb in the presence of the first mAb was determined by comparing the maximal signal of the second mAb after the first mAb was added to the maximum signal of the second mAb alone. mAbs were considered non-competing if maximum binding of the second mAb was ≥66% of its un-competed binding. A level between 33% and 66% of its un-competed binding was considered intermediate competition, and ≤33% was considered competing.

Enzyme-linked immunosorbent assay (ELISA) measurement. For recombinant protein capture ELISA, 384-well plates (Greiner) were treated with 2 μg/mL of antigen overnight at 4 °C. The plates were blocked for one hour with 2% nonfat milk (Biorad) supplemented with 2% goat serum (ThermoFisher) in PBS with 0.05% Tween-20 (PBS-T). Plates were washed three times with water, and 25 μL of primary mAbs were applied to wells for one hour. Plates were washed with water three times before applying 25 μL of the secondary antibody (goat anti-mouse IgG-AP, Southern Biotech #1030-04) at a dilution of 1:4,000 in blocking solution. Binding of CR6261 was analyzed using a goat anti-human IgG Fc-AP antibody (Meridian Life Science, #W99008A). After a one-hour incubation, the plates were washed five times with PBS-T, and 25 μL of phosphatase substrate solution (1 mg/mL phosphatase substrate in 1 M Tris base) was added to each well. The plates were incubated at room temperature for 60 min before reading the opti-

cal density at 405 nm on a Biotek xs plate reader. Data were analyzed in GraphPad prism using a nonlinear regression curve fit (agonist).

3. Crystallization and structure determination of the COBRA2 HA protein

To crystallize the COBRA2Y91F protein, the sample was subjected to size exclusion chromatography (S200, 16/600, GE Healthcare Life Sciences) in 50 mM Tris pH 7.5, 50 mM NaCl. The fractions corresponding to a trimeric protein were concentrated to 10 mg/mL and crystallization trials were prepared on a TTPLabTech Mosquito Robot in sitting-drop MRC-2 plates (Hampton Research) in 0.3 μL drops mixed 1:1 with the precipitant. Several commercially available crystallization screens were used in the crystallization trials. Crystals were obtained in the Molecular Dimensions SG1 HT-96 screen in conditions E3, B12, D10, F10 and E10. The best diffracting crystals were obtained in 30% PEG 400, 200 mM $MgCl_2 \cdot 6H_2O$, and 100 mM HEPES pH 7.5. Crystals were harvested and cryo-protected with 20% glycerol in the mother liquor before being flash frozen in liquid nitrogen. X-ray diffraction data were collected at the Advanced Photon Source SER-CAT beamline 22-ID-D. Data were indexed and scaled using XDS [24]. Aimless [25] was then used to merge and truncate the data, and generate a 5% fraction for R_{free} calculations. A molecular replacement solution was obtained in Phaser [26] using the H5 Vietnam/04 crystal structure (PDB 2FK0). The crystal structure of the complex was completed by manually building in COOT [27] onto a truncated polyalanine model of 2FK0, followed by subsequent rounds of deletions, manual rebuilding, and refinement in Phenix [26]. The data collection and refinement statistics are shown in Table 1.

Table 1
Data collection and refinement statistics.

Data collection	
Beamline	SER-CAT 22-ID-D
Number of crystals	1
Space group	R 3 2 :H
Cell dimensions	
a, *b*, *c* (Å)	101.5 101.5 450.1
a, b, g (°)	90 90 120
Resolution (Å)	48.08–2.8 (2.9–2.8)
R-merge	0.1277 (1.534)
CC1/2	0.996 (0.961)
CC*	0.999 (0.990)
I/σI	14.73 (1.54)
Completeness (%)	99.10 (98.83)
Redundancy	11.1 (11.7)
Refinement	
Resolution	48.08–2.8
No. unique reflections	22,588 (2211)
R_{work}/R_{free}	0.2352/0.2735
No. atoms	
Protein	3927
Ligand	129
B-factors	
Protein	90.42
Ligand	124.62
R.m.s. deviations	
Bond lengths (Å)	0.011
Bond angles (°)	1.35
Ramachandran statistics	
Favored regions (%)	91.99
Allowed regions (%)	8.01
Outliers (%)	0

* Values in parentheses are for highest-resolution shell.

4. Results

COBRA2 biochemical characterization. Current seasonal influenza vaccines rely on live or split, inactivated virus using naturally-occurring HA sequences. As progress is made toward a universal influenza vaccine using designer-antigens, the conformational quality of these antigens must be confirmed to ensure their effectiveness. The COBRA2 antigen was the first published antigen using the COBRA methodology [16]. Of the H5 influenza HA proteins, the most well-studied are those closely related to the A/Vietnam/1203/04 virus. As amino acid combinations are present in the H5 COBRA2 HA protein that are not naturally occurring, we sought to biochemically analyze the COBRA2 HA protein to determine the overall fold and conformation. Analysis of purified protein by SDS-PAGE indicated the protein migrates as a monomer due to disruption of the trimer structure from denaturing running conditions (Fig. 1A). No major differences were observed between the COBRA2 HA protein and the COBRA2Y91F mutant proteins used in crystallization trials. Upon addition of reducing agent, two bands were observed for the HA_1 and HA_2 protein fragments as expected, indicative of disruption of the disulfide bond tethering the two fragments together, and of proper cleavage of the HA protein. As native HA on the surface of influenza viruses are trimeric, the COBRA2 HA protein contains a foldon trimerization domain to encourage trimerization of cleaved H5 monomers. We performed size exclusion chromatography on the COBRA2 HA protein to confirm the foldon domain was correctly functioning to stabilize the COBRA2 HA trimer. As compared to a molecular weight standard, the protein eluted at an apparent molecular weight of 379 kDa, as compared to the 189 kDa size expected of a HA trimer (Fig. 1B). The larger size for HA was previously reported for HA trimers analyzed by size exclusion chromatography and multi-angle light scattering, consistent with our results [28]. Higher molecular weight oligomeric protein was also obtained depending on the protein batch. The trimeric protein was analyzed by negative-stain electron microscopy and was observed to be primarily single particles consistent with the shape of a HA trimer (Fig. 1C). To determine the general antigenic characteristics of the COBRA2 protein, we examined the binding properties of several mouse mAbs, although only two showed significant binding on the Octet system, a mouse-derived head-binding mAb, AT159.134.119, and a human-derived broadly-neutralizing stem-binding mAb CR6261 [29]. Both mAbs rapidly bound to the COBRA2 protein and had limited off rates, suggesting their high affinity for the COBRA2 protein (Fig. 1C). Furthermore, we performed competition of these two mAbs to ensure the head and stem of the COBRA2 HA protein were antigenically intact, and as expected, no competition was observed amongst the two mAbs for COBRA2 HA protein binding. Overall, these data suggest the COBRA2 HA antigen is properly cleaved, trimeric, and has structurally correct head and stem regions. As the COBRA2 HA protein was expressed in HEK293F cells, substantial glycosylation was expected. We monitored the glycosylation by utilizing the deglycosylating enzyme PNGase F. Upon addition of PNGase F, a mobility shift in the SDS-PAGE was observed in both the denatured and nondenatured deglycosylation protocols. The denaturing protocol incorporates DTT, thus breakup of the HA molecule into two fragments was also observed.

Antibody characterization. As the COBRA2 HA protein has substantial amino acids alterations compared to naturally-occurring H5 HA sequences, the antigenic characteristics of the H5 protein were probed using a previously discovered panel of mouse mAbs generated to the H5 Vietnam virus (Fig. 2A and B). Each mAb was tested for binding to the COBRA2, COBRA2Y91F mutant, A/Indonesia/5/05, A/Vietnam/1203/04 HA1, A/Anhui/1/05, and A/Whooper Swan/Mongolia/05 HA proteins. All mAbs bound with a similar EC_{50} to the A/Vietnam/1203/04 and A/Whooper Swan/Mongolia/05 proteins. mAbs 1C10 and DPJY02 did not bind to

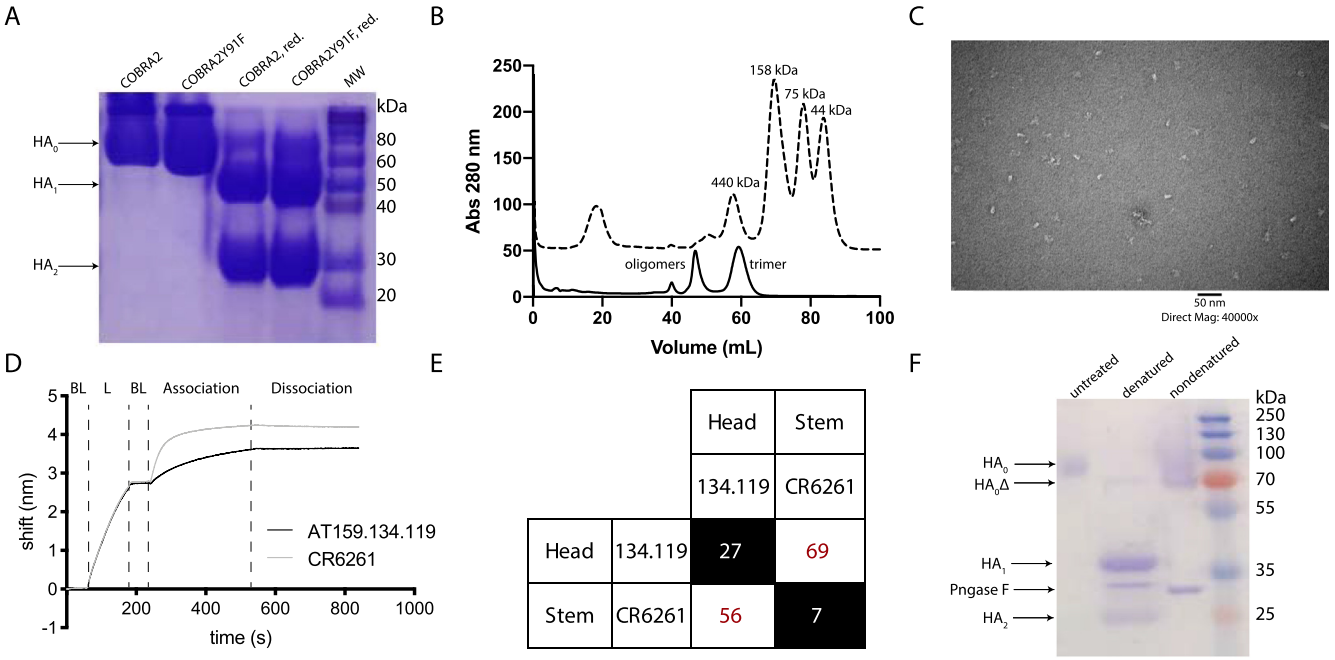

Fig. 1. Biochemical characterization of the COBRA2 antigen. (A) SDS-PAGE of COBRA2 and COBRA2Y91F. Each sample was examined in the presence and absence of β-mercaptoethanol. Each protein runs as a monomer, with the reduced samples showing two bands corresponding to HA_1 and HA_2 fragments. (B) Size exclusion chromatography of the COBRA2Y91F protein. The protein migrates as a trimer on the HiLoad S200 16/600 column. (C) Negative-strain electron microscopy image of the COBRA2 protein. The protein consists primarily of single particles resembling a trimeric HA molecule. (D) Biolayer interferometry analysis showing two mAbs, AT159.134.119 and CR6261 binding to the COBRA2Y91F protein with limited dissociation. Dashed lines indicate each step in the experiment, BL (baseline), L (loading). (E) Competition analysis between AT159.134.119 and CR6261 on the COBRA2Y91F protein. mAbs were considered non-competing if maximum binding of the second mAb was ≥66% of its uncompeted binding (white boxes). A level between 33% and 66% of its un-competed binding was considered intermediate competition (none observed), and ≤33% was considered competing (black boxes). (F) Mobility shift assay by SDS-PAGE showing a shift in the molecular weight of the COBRA2 protein after treatment with PNGase F. The denatured protocol incorporated DTT, which causes dissociation of the HA protein due to disruption of disulfide bonds. The nondenatured protocol utilized reducing agent-free buffer over 24 h. PNGase F is visible in the gel and the size is based on the manufacturer's protocols.

any other construct, suggesting the epitope for these mAbs is only found on the A/Vietnam/1203/04 and A/Whooper Swan/Mongolia/06 HA protein. mAbs 464E11 was found to bind to all constructs except A/Anhui/1/05, suggesting the epitope for 464E11 is altered in this strain. mAbs AT159.257.173 and AT159.134.119 bound to all constructs tested, likely to a conserved epitope on the head of the HA protein. The binding patterns of the COBRA2 and COBRA2Y91F proteins are identical to the A/Indonesia/5/05 HA protein. These data suggest the COBRA2 protein is antigenically similar to H5 HA proteins from which the COBRA2 sequence was formulated. In addition, we examined the binding of a HA stem-specific human antibody, CR6261, which was observed to bind to all full-length HA constructs as expected due to sequence conservation at the stem region of HA molecules. No binding was observed to the A/Vietnam/1203/04 HA1 construct, as this protein lacks a full stem region.

Overall structural features of the COBRA2Y91F protein. Crystal structures of A/Vietnam/1203/04 strains have been determined alone [30–32] and in complex with neutralizing mAbs [33–36]. In addition, crystal structures of A/Indonesia/5/05 [37], and A/Anhui/1/05 [30,38] have been determined. To identify the structural features of the COBRA2 HA antigen, we attempted to crystallize the native COBRA2 antigen, but were unsuccessful. We were successful in crystallizing the COBRA2Y91F HA protein, which contains the Y91F mutation to abrogate sialic acid binding, and this construct crystallized well in multiple conditions. The crystal structure was solved to 2.8 Å with an R_{work}/R_{free} of 0.2352 / 0.2735 (Fig. 3A, Table 1). The COBRA2Y91F HA protein contained a monomer in the asymmetric unit, and crystallized as a trimer in the biological unit, similar to our observations from size exclusion chromatography and negative-strain electron microscopy. The overall crystal structure of the COBRA2 protein aligns well to previously determined crystal structures A/Vietnam/1203/04, A/Anhui/1/05, and A/Indonesia/5/05 with RMS from PyMOL alignments being 0.382 (3154 atoms aligned), 0.669 (3099 atoms aligned), and 0.513 (3046 atoms aligned), respectively (Fig. 3B). The A/Anhui/1/05 HA crystal structure is the most divergent from the others due to slight changes in loop placement throughout the HA molecule. These data indicate the recombinantly-expressed COBRA2 protein derived from HEK293F cells is structurally similar to recombinantly expressed HA antigens with naturally occurring extracellular domain sequences.

Consensus residues. The amino acid residues that differ between COBRA2 HA and the three H5 HA strains A/Vietnam/1203/04, A/Indonesia/5/05, and A/Anhui/1/05 are predominantly focused on the HA head domain, since this region is the most variable among circulating influenza strains (Fig. 4A and B). The COBRA2 HA protein contains residues from all three comparing strains, with 1–2 differences among each position between the four HA sequences (Fig. 4A and C). To identify if major structural changes at each amino acid position were present in the COBRA2 HA protein, we compared the structural overlay of the COBRA2Y91F HA crystal structure to that of the three corresponding H5 HA strains (Fig. 4C). Overall, there were no major differences among amino acid side chains for HA strains containing identical residues to the COBRA2Y91F HA protein. This structural homology was observed across amino acid chemical groups, including flexible proline residues, and charged and hydrophobic amino acids. Slight differences were observed for Arg residues at position 189 and 310, however, the difference at position 310 is due to alternative confirmations being present in the electron density of the COBRA2Y91F crystal structure.

Glycosylation of the recombinant COBRA2 HA antigen. The COBRA2 HA molecule has predicted N-linked glycosylation sites

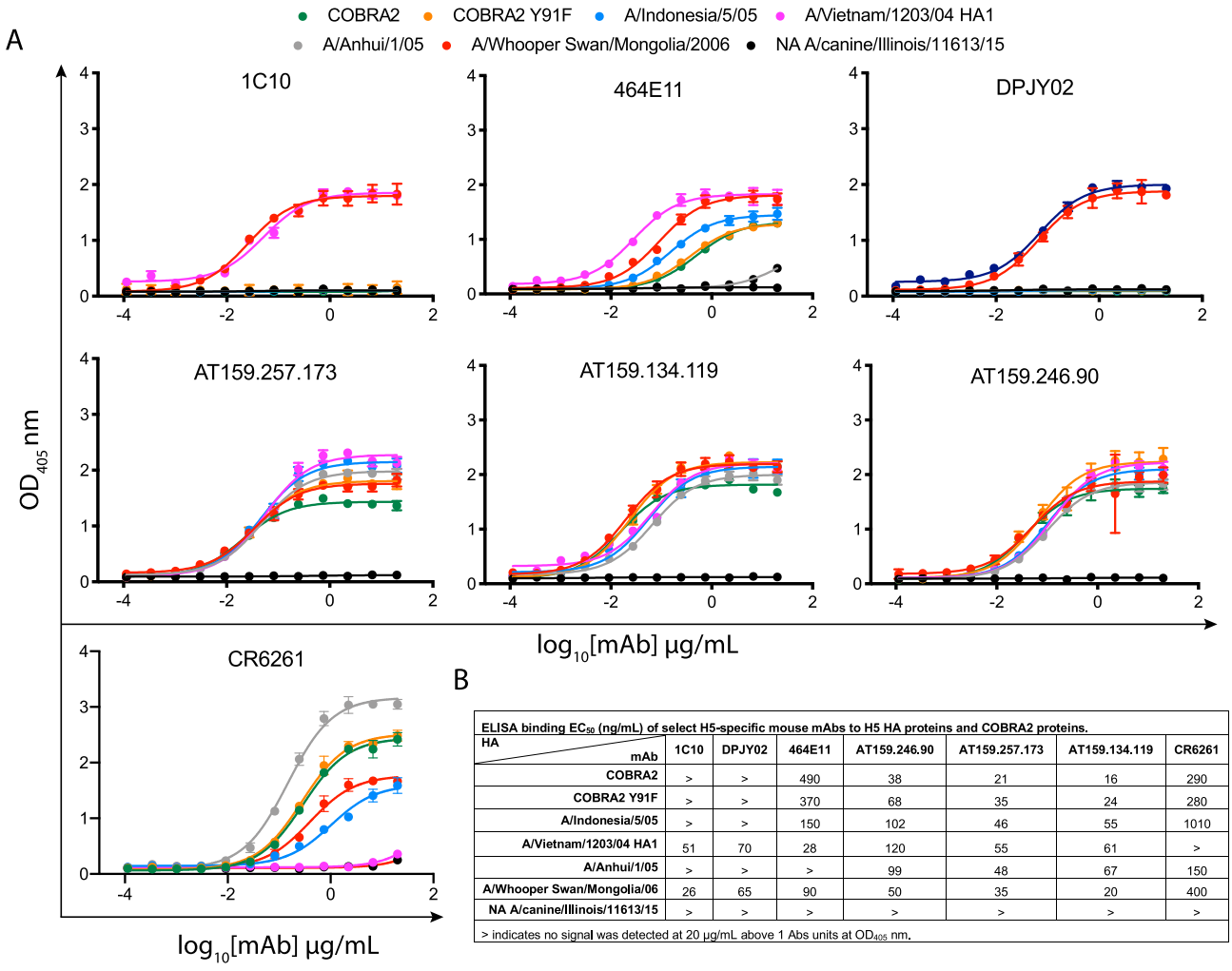

ELISA binding EC_{50} (ng/mL) of select H5-specific mouse mAbs to H5 HA proteins and COBRA2 proteins.

HA \ mAb	1C10	DPJY02	464E11	AT159.246.90	AT159.257.173	AT159.134.119	CR6261
COBRA2	>	>	490	38	21	16	290
COBRA2 Y91F	>	>	370	68	35	24	280
A/Indonesia/5/05	>	>	150	102	46	55	1010
A/Vietnam/1203/04 HA1	51	70	28	120	55	61	>
A/Anhui/1/05	>	>	>	99	48	67	150
A/Whooper Swan/Mongolia/06	26	65	90	50	35	20	400
NA A/canine/Illinois/11613/15	>	>	>	>	>	>	>

> indicates no signal was detected at 20 µg/mL above 1 Abs units at OD_{405} nm.

Fig. 2. Antigenic characterization of the COBRA2 antigen. (A) ELISA curves of serially diluted mouse mAbs binding to COBRA2, COBRA2Y91F, A/Indonesia/5/05, A/Vietnam/1203/04 HA1, A/Anhui/1/05, and A/WhooperSwan/Mongolia/2006 HA proteins. The A/canine/Illinois/11613/15NA protein was used as a negative binding control. Each data point is the average of four replicates, and error bars indicate the standard deviation. (B) EC_{50} values calculated from the curves in (A). >indicates a signal greater than 1.0 was not observed for the 20 µg/mL starting concentration.

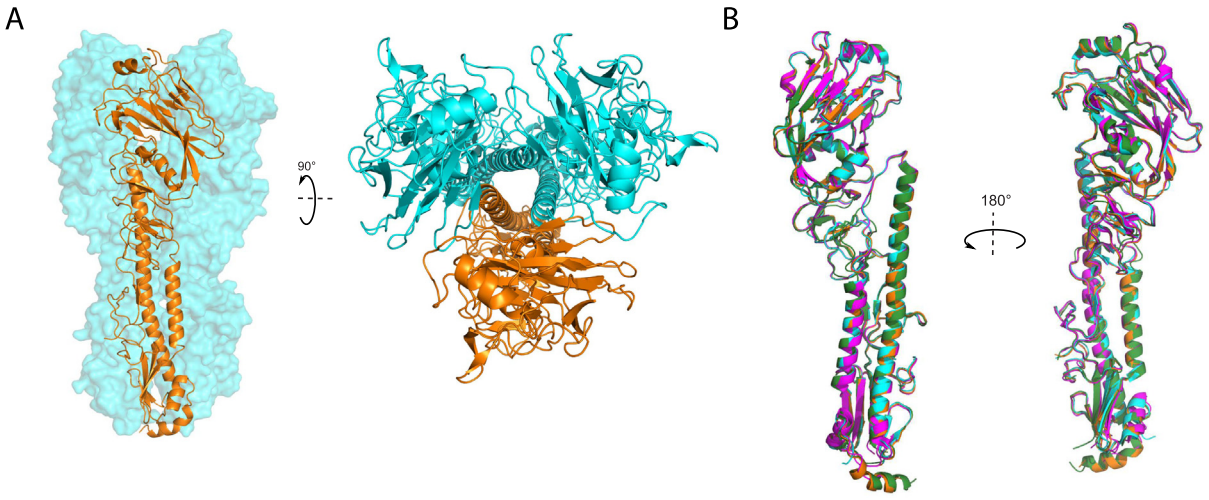

Fig. 3. Crystal structure of the COBRA2Y91F protein. (A) Overall structure of the COBRA2Y91F protein. The protein crystallized as a trimer in the biological unit, and a single monomer was in the asymmetric unit. Two monomers are shown in surface representation, and one monomer is shown in cartoon form. The protein is shown rotated 90° looking from the top down. (B) Crystal structures of naturally occurring H5 influenza HA sequences are overlaid on the COBRA2Y91F structure. The COBRA2Y91F protein is shown in orange, the A/Vietnam/1203/04 structure is shown in cyan, the A/Anhui/1/05 is shown in green, and the A/Indonesia/5/05 is shown in magenta. (For interpretation of the references to colour in this figure legend, the reader is referred to the web version of this article.)

A

Position	86	94	124	129	138	140	141	155	162	174	181	189	200	212	227	263	265	269	282	310
COBRA2	A	N	D	S	Q	S	P	N	R	V	P	R	V	K	E	A	M	L	I	R
A/Anhui/1/2005	A	N	D	S	Q	T	P	N	R	I	S	K	V	K	D	S	V	V	I	K
A/Indonesia/5/2005	T	S	D	S	L	S	P	S	K	V	P	R	I	K	E	A	M	L	M	R
A/Vietnam/1203/2004	V	D	S	L	Q	K	S	S	R	V	P	K	V	R	E	T	M	L	M	R

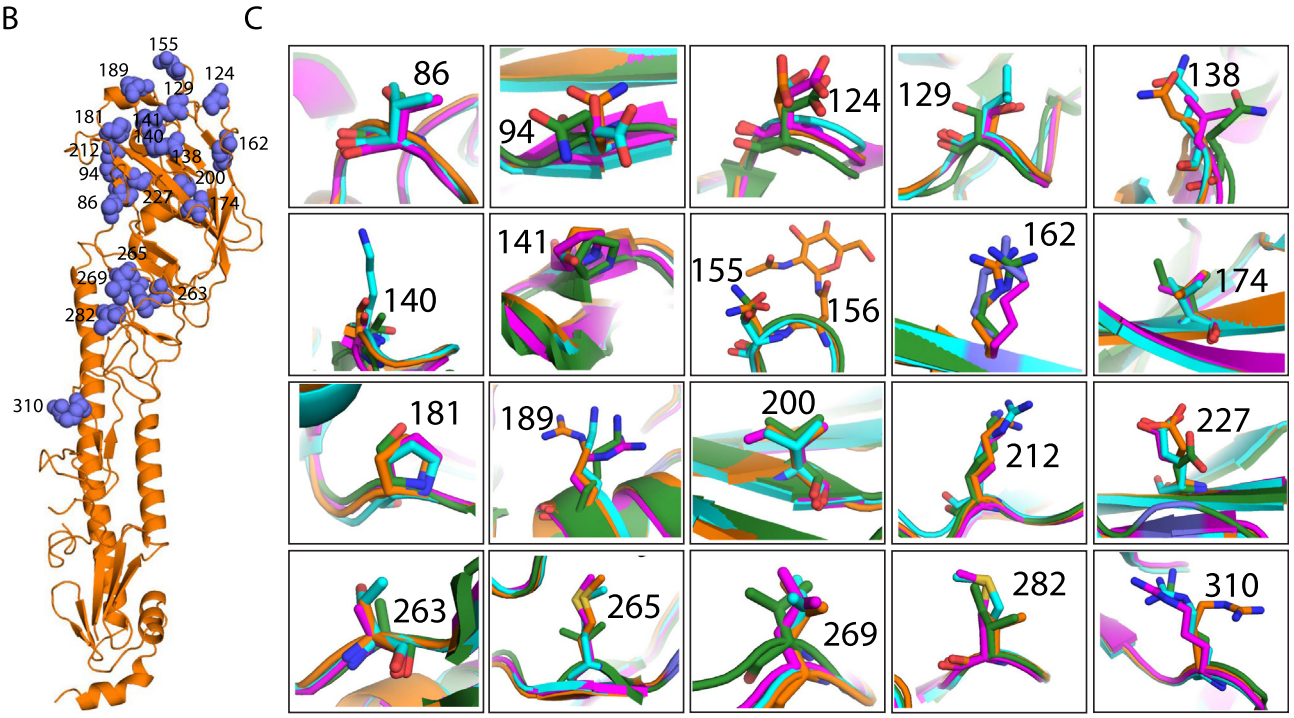

Fig. 4. Fine structural comparison of the COBRA2Y91F protein to naturally occurring sequences. (A) Sequence comparisons between the COBRA2 protein and A/Anhui/1/05, A/Indonesia/5/05, and A/Vietnam/1203/04. (B) The crystal structure of the COBRA2Y91F protein with residues highlighted in blue spheres that differ among the four sequences shown in (A). (C) Each residue highlighted in (B) is shown in stick form to compare amino acid differences among the four protein sequences. (For interpretation of the references to colour in this figure legend, the reader is referred to the web version of this article.)

at residues 10, 11, 23, 154, 165, 193, 286, and 484 based on the NetNGlyc 1.0 Server, and overall protein glycosylation was observed by treatment with PNGase F (Fig. 1F). Homologous residues are predicted to be glycosylated in the A/Vietnam/1203/04, A/Indonesia/5/05, and A/Anhui/1/05 HA sequences. As we expressed the protein in HEK293F cells, and did not modify the protein glycosylation before crystallization, N-linked glycans were visible throughout the electron density, including one residue at Asn23, two residues at Asn165, one residue at Asn154, and two residues at Asn484. As the COBRA2 HA sequence is derived from naturally occurring influenza HA sequences, it is unlikely that N-linked glycosylation positions would be affected. We observed glycans at predicted positions in the COBRA2 HA crystal structure as expected. Residues 154-155 consists of two adjacent Asn side chains based on the predominant position of Asn at these positions in 2004–2006 circulating strains derived from human infections. HA proteins from A/Vietnam/1203/04 and A/Indonesia/5/05 H5N1 strains contain a Ser residue at position 155, which is different than the Asn at this position in the COBRA2 and A/Anhui/1/05 HA sequences. Although there are two adjacent Asn residues, we observed glycosylation in the electron density at only position 155.

5. Discussion

The development of a universal influenza vaccine is of high priority to the medical and scientific community [39]. Several candidates are under investigation, including antigens derived via the COBRA methodology. Our goal in this study was to structurally characterize the COBRA2 HA antigen that was previously developed for H5 influenza infection to increase the breadth of responses induced by vaccination [16]. The COBRA2 HA protein is structurally homologous to crystal structures determined for H5 HA molecules from the similar time period, including A/Vietnam/1203/04, A/Indonesia/5/05, and A/Anhui/1/05 [30,31,37]. The COBRA2 HA protein contains no major structural changes among consensus amino acid residues and appears glycosylated based on a mobility shift assay and electron density surrounding Asn residues in the electron density map, which correspond with N-linked glycosylation prediction software. The mechanism by which the COBRA methodology elicits a broadly neutralizing response has yet to be definitively determined, although experiments are being conducted using monoclonal antibody isolation to assist in identifying the basis for the increased breadth. The data presented here suggest the COBRA2 HA molecule displays antigenic sites of numerous HA sequences, based on the structural similarity of the COBRA2 HA molecule to other structurally determined HA sequences. For example, amino acid residue 129 may present Asp in the context of a complex epitope being recognized by a B cell, which would generate antibodies against A/Anhui/1/05 and A/Indonesia/5/05, but not A/Vietnam/1203/04. Similarly, amino acid position 181 would generate antibodies to A/Indonesia/5/05 and A/Vietnam/1203/04, but not A/Anhui/1/05, due to differences in amino acids at this position. Based on this idea, our hypothesis is that the COBRA2 HA antigen elicits strain-specific mAbs to a broad number of epitopes. Although this is a plausible hypothesis based on our data, we cannot rule out that the COBRA2 HA antigen is eliciting broadly neutralizing monoclonal antibodies, as B cells likely recognize conformational epi-

topes incorporating numerous amino acid residues present in the COBRA HA sequence. Further investigation by monoclonal antibody isolation and characterization will address this question for the COBRA2 HA antigen and for COBRA antigens we are currently studying for additional influenza subgroups.

Declaration of Competing Interest

The authors declare that they have no known competing financial interests or personal relationships that could have appeared to influence the work reported in this paper.

Acknowledgements

These studies were supported by the University of Georgia Office of Vice President for Research, Department of Infectious Diseases, and Center for Vaccines and Immunology. X-ray data were collected at the Southeast Regional Collaborative Access Team (SER-CAT) 22-ID beamline at the Advanced Photon Source, Argonne National Laboratory. SER-CAT is supported by its member institutions (see www.ser-cat.org/members.html), and equipment grants (S10_RR25528 and S10_RR028976) from the National Institutes of Health. Use of the Advanced Photon Source was supported by the U.S. Department of Energy, Office of Science, Office of Basic Energy Sciences, under Contract No. W-31-109-Eng-38. We are grateful to the International Reagent Resource (IRR) for mAbs AT159.246.90, AT159.257.173, and AT159.134.119, and the A/Vietnam/1203/04, A/Anhui/1/05, and A/Indonesia/5/05 proteins, and to the Biodefense and Emerging Infections Research Resources Repository (BEI Resources) for the influenza antibody reagents DPJY02, 464E11, 6B4. We thank the CVI Antibody Core for use of the OctetRED384 system. The structure factors and structure coordinates were deposited to the Protein Data Bank under accession code 6NTF. TMR is supported, in part, from the Georgia Research Alliance as an Eminent Scholar. JJM is supported by the National Institutes of Health grant 1K01OD026569 and 1R01AI14386501.

References

[1] Saunders-Hastings P, Krewski D. Reviewing the history of pandemic influenza: Understanding patterns of emergence and transmission. Pathogens 2016;5:66. https://doi.org/10.3390/pathogens5040066.
[2] Taubenberger JK, Morens DM. 1918 Influenza: The mother of all pandemics. Emerg Infect Dis 2006;12:15–22. https://doi.org/10.3201/eid1201.050979.
[3] Girard MP, Tam JS, Assossou OM, Kieny MP. The 2009 A (H1N1) influenza virus pandemic: A review. Vaccine 2010;28:4895–902. https://doi.org/10.1016/j.vaccine.2010.05.031.
[4] WHO. Cumulative number of confirmed human cases for avian influenza A (H5N1) reported to WHO, 2003-2019 2015; https://ww:5–6. doi:10.1016/j.archoralbio.2009.02.002.
[5] WHO. Antigenic and genetic characteristics of zoonotic influenza viruses and development of candidate vaccine viruses for pandemic preparedness. Relev Epidemiol Hebd 2015;90:261–78. https://doi.org/10.1111/irv.12324/epdf.
[6] VanderWaal K, Sorley EJ, Wells SJ, Sundaram ME, Kromm MM, Bender J, et al. Epidemiologic investigation of highly pathogenic H5N2 avian influenza among upper Midwest U.S. turkey farms, 2015. Avian Dis 2017;61:198–204. https://doi.org/10.1637/11543-112816-reg.1.
[7] Choi K-S, Jeong SC, Lee Y-N, Jeong O-M, Joh S-J, Park S-C, et al. Multiple novel H5N6 highly pathogenic avian influenza viruses, South Korea, 2016. Infect Genet Evol 2017;51:21–3. https://doi.org/10.1016/j.meegid.2017.03.005.
[8] Peiris JSM, Cowling BJ, Wu JT, Feng L, Guan Y, Yu H, et al. Interventions to reduce zoonotic and pandemic risks from avian influenza in Asia. Lancet Infect Dis 2016;16:252–8. https://doi.org/10.1016/S1473-3099(15)00502-2.
[9] Adlhoch C, Zohari S, Grund C, Zdravkova A, Buda S, Popescu R, et al. Highly pathogenic avian influenza A(H5N8) outbreaks: protection and management of exposed people in Europe, 2014/15 and 2016. Euro Surveill 2016;21:1–7. https://doi.org/10.2807/1560-7917.es.2016.21.49.30419.
[10] Herfst S, Schrauwen EJA, Linster M, Chutinimitkul S, de Wit E, Munster VJ, et al. Airborne transmission of influenza A/H5N1 virus between ferrets. Science 2012;336:1534–41. https://doi.org/10.1126/science.1213362.
[11] Chen LM, Davis CT, Zhou H, Cox NJ, Donis RO. Genetic compatibility and virulence of reassortants derived from contemporary avian H5N1 and human H3N2 influenza A viruses. PLoS Pathog 2008;4:1–11. https://doi.org/10.1371/journal.ppat.1000072.
[12] Mulatti P, Fusaro A, Scolamacchia F, Zecchin B, Azzolini A, Zamperin G, et al. Integration of genetic and epidemiological data to infer H5N8 HPAI virus transmission dynamics during the 2016–2017 epidemic in Italy. Sci Rep 2018;8:18037. https://doi.org/10.1038/s41598-018-36892-1.
[13] Takahashi K, Komatsuzaki J, Takahata Y. Evolution, global spread, and pathogenicity of highly pathogenic avian influenza H5Nx clade 2.3.4.4. J Vet Sci 2017;18:269–80. https://doi.org/10.1252/jcej.13we358.
[14] Antigenic and genetic characteristics of influenza A (H5N1) and influenza A (H9N2) viruses for the development of candidate vaccine viruses for pandemic preparedness Influenza A (H5N1). Wkly Epidemiol Rec 2011:93–100.
[15] Belongia EA, Simpson MD, King JP, Sundaram ME, Kelley NS, Osterholm MT, et al. Variable influenza vaccine effectiveness by subtype: a systematic review and meta-analysis of test-negative design studies. Lancet Infect Dis 2016;16:942–51. https://doi.org/10.1016/S1473-3099(16)00129-8.
[16] Giles BM, Ross TM. A computationally optimized broadly reactive antigen (COBRA) based H5N1 VLP vaccine elicits broadly reactive antibodies in mice and ferrets. Vaccine 2011;29:3043–54. https://doi.org/10.1016/j.vaccine.2011.01.100.
[17] Carter DM, Darby CA, Lefoley BC, Crevar CJ, Alefantis T, Oomen R, et al. Design and characterization of a computationally optimized broadly reactive hemagglutinin vaccine for H1N1 influenza viruses. J Virol 2016;90:4720–34. https://doi.org/10.1128/JVI.03152-15.
[18] Sautto GA, Kirchenbaum GA, Ecker JW, Bebin-Blackwell A-G, Pierce SR, Ross TM. Elicitation of broadly protective antibodies following infection with influenza viruses expressing H1N1 computationally optimized broadly reactive hemagglutinin antigens. ImmunoHorizons 2018;2:226–37. https://doi.org/10.4049/immunohorizons.1800044.
[19] Giles BM, Bissel SJ, DeAlmeida DR, Wiley CA, Ross TM. Antibody breadth and protective efficacy are increased by vaccination with computationally optimized hemagglutinin but not with polyvalent hemagglutinin-based H5N1 virus-like particle vaccines. Clin Vacc Immunol 2012;19:128–39. https://doi.org/10.1128/CVI.05533-11.
[20] Crevar CJ, Carter DM, Lee KYJ, Ross TM. Cocktail of H5N1 COBRA HA vaccines elicit protective antibodies against H5N1 viruses from multiple clades. Hum Vaccines Immunother 2015;11:572–83. https://doi.org/10.1080/21645515.2015.1012013.
[21] Allen JD, Owino SO, Carter DM, Crevar CJ, Reese VA, Fox CB, et al. Broadened immunity and protective responses with emulsion-adjuvanted H5 COBRA-VLP vaccines. Vaccine 2017;35:5209–16. https://doi.org/10.1016/j.vaccine.2017.07.107.
[22] Whittle JRR, Wheatley AK, Wu L, Lingwood D, Kanekiyo M, Ma SS, et al. Flow cytometry reveals that H5N1 vaccination elicits cross-reactive stem-directed antibodies from multiple Ig heavy-chain lineages. J Virol 2014;88:4047–57. https://doi.org/10.1128/JVI.03422-13.
[23] Kirchenbaum GA, Allen JD, Layman TS, Sautto GA, Ross TM. Infection of ferrets with influenza virus elicits a light chain–biased antibody response against hemagglutinin. J Immunol 2017;199:3798–807. https://doi.org/10.4049/jimmunol.1701174.
[24] Kabsch W. Xds. Acta Cryst 2010;66:125–32. https://doi.org/10.1107/S0907444909047337.
[25] Evans PR, Murshudov GN. How good are my data and what is the resolution? Acta Cryst 2013;69:1204–14. https://doi.org/10.1107/S0907444913000061.
[26] Adams PD, Afonine PV, Bunkóczi G, Chen VB, Davis IW, Echols N, et al. PHENIX: a comprehensive Python-based system for macromolecular structure solution. Acta Cryst 2010;66:213–21. https://doi.org/10.1107/S0907444909052925.
[27] Emsley P, Cowtan K. Coot: model-building tools for molecular graphics. Acta Cryst 2004;60:2126–32. https://doi.org/10.1107/S0907444904019158.
[28] Macioła AK, Pietrzak MA, Kosson P, Czarnocki-Cieciura M, Śmietanka K, Minta Z, et al. The length of N-glycans of recombinant H5N1 hemagglutinin influences the oligomerization and immunogenicity of vaccine antigen. Front Immunol 2017;8:444. https://doi.org/10.3389/fimmu.2017.00444.
[29] Koudstaal W, Koldijk MH, Brakenhoff JPJ, Cornelissen LAHM, Weverling GJ, Friesen RHE, et al. Pre- and postexposure use of human monoclonal antibody against H5N1 and H1N1 influenza virus in mice: Viable alternative to oseltamivir. J Infect Dis 2009;200:1870–3. https://doi.org/10.1086/648378.
[30] Shore DA, Yang H, Balish AL, Shepard SS, Carney PJ, Chang JC, et al. Structural and antigenic variation among diverse clade 2 H5N1 viruses e75209. PLoS ONE 2013;8. https://doi.org/10.1371/journal.pone.0075209.
[31] Xiong X, Coombs PJ, Martin SR, Liu J, Xiao H, McCauley JW, et al. Receptor binding by a ferret-transmissible H5 avian influenza virus. Nature 2013;497:392–6. https://doi.org/10.1038/nature12144.
[32] Stevens J, Blixt O, Tumpey TM, Taubenberger JK, Paulson JC, Wilson IA. Structure and receptor specificity of the hemagglutinin from an H5N1 influenza virus. Science 2006;312:404–9.
[33] Xiong X, Corti D, Liu J, Pinna D, Foglierini M, Calder LJ, et al. Structures of complexes formed by H5 influenza hemagglutinin with a potent broadly neutralizing human monoclonal antibody. PNAS 2015;112:9430–5. https://doi.org/10.1073/pnas.1510816112.
[34] Kallewaard NL, Corti D, Collins PJ, Neu U, McAuliffe JM, Benjamin E, et al. Structure and function analysis of an antibody recognizing all influenza A subtypes. Cell 2016;166:596–608. https://doi.org/10.1016/j.cell.2016.05.073.
[35] Winarski KL, Thornburg NJ, Yu Y, Sapparapu G, Crowe JE, Spiller BW. Vaccine-elicited antibody that neutralizes H5N1 influenza and variants binds the receptor site and polymorphic sites. PNAS 2015;112:9346–51. https://doi.org/10.1073/pnas.1502762112.

[36] Ekiert DC, Bhabha G, Elsliger M, Friesen RHE, Jongeneelen M, Throsby M, et al. Antibody recognition of a highly conserved influenza virus epitope. Science 2009;1857:246–51.
[37] Zhang W, Shi Y, Lu X, Shu Y, Qi J, Gao GF. An airborne transmissible avian influenza H5 hemagglutinin seen at the atomic level. Science 2013;340:1463–7.
[38] Zuo T, Sun J, Wang G, Jiang L, Zuo Y, Li D, et al. Comprehensive analysis of antibody recognition in convalescent humans from highly pathogenic avian influenza H5N1 infection. Nat Commun 2015;6:1–12. https://doi.org/10.1038/ncomms9855.
[39] Erbelding EJ, Post DJ, Stemmy EJ, Roberts PC, Augustine AD, Ferguson S, et al. A universal influenza vaccine: The strategic plan for the national institute of allergy and infectious diseases. J Infect Dis 2018;218:347–54. https://doi.org/10.1093/infdis/jiy103.